METHODOLOGY FOR ESTABLISHING FRICTIONAL REQUIREMENTS

Joel M. Zuieback, Science Applications, Inc.,
El Segundo, California 90245

The nature of the wet-pavement skidding accident problem is briefly discussed. A cursory review of the traffic accident literature is given to highlight the roadway geometric and driver maneuver performance specific nature of the problem. A conceptual methodology to establish cost-effective frictional requirements is presented. This methodology is based upon the calculation of a margin of safety (MOS) defined as the difference between available tire-pavement friction and the level of driver demand for friction. Models to calculate the level of available tire-pavement friction and the level of frictional demand as a function of site specific traffic operational characteristics, roadway geometry, and surface characteristics are discussed, and an example is given for the case of two-lane passing.

Introduction

Rising mean traffic speeds and increasing traffic volumes on many highway facilities have resulted in an ever increasing potential for wet pavement skidding accident occurrence. The problem is depicted in Figure 1 where the general relationship between available tire-pavement frictional force and driver demand for that frictional force are shown. The fundamental dependence upon speed, as shown in the figure, arises from the fact that on wet pavements, the tire-pavement contact area is determined by the efficiency with which the tire can expel water from that area. Viscocity and other effects cause this efficiency to degrade at higher speeds — the tire is unable to maintain a dry contact area. In the limit, at high speed, the tire hydroplanes if there is sufficient water film thickness. As will be discussed, the determination of tire-pavement frictional levels is highly dependent upon site specific considerations including the environment, traffic operational characteristics, and most importantly, vehicle maneuver determining roadway geometry. Before discussing these factors, some background on the skidding accident problem is given.

Rizenbergs (1), reports the results of an accident correlation study which indicates that the ratio of wet-pavement accidents to all reported accidents (wet-pavement accident ratio) on high speed facilities in Kentucky is between 0.15 and 0.25. A similar study conducted in Virginia (2) in 1958 indicated a wet-pavement accident ratio of between 0.2 and 0.4.

The accident statistics reported above indicate wet-pavement accident rates but do not differentiate skidding accidents from other wet-pavement accidents. Hankins (3) reports the results of a detailed accident investigation and analysis study in which he found that 63.6 percent of all wet-pavement accidents in Texas in recent years were attributable to skidding. Hankins also was able to demonstrate the fact that different accident rates could be attributed to different vehicle maneuver situations. In particular, his data indicate that 40 percent of wet-pavement accidents involve a cornering action of the vehicle, where a cornering action is also defined to include passing maneuvers. Kummer and Meyer (4) report a survey of six states where the fraction of wet-pavement accidents attributable to skidding was determined. The results of that survey are given below:

Skidding Accidents/Wet Pavement Accidents (5)

	1960	1961	1962	1963	1964	1965
Arizona	--	--	1.4	0.5	0	--
Connecticut	17.2	18.2	15.6	19.6	13.6	11.8
Louisiana	32.6	34.1	11.7	13.5	2.4	--
Maine	--	--	--	--	23.4	--
Montana	12.0	7.5	0.7	4.6	1.5	--
Wyoming	--	0.9	1.4	0.9	20.3	--

Numerous other investigations have obtained results which suggest that the occurrence of skidding accidents is maneuver specific. Smith(5), in his summary of all NCHRP research, states the conclusion that intersections and curves are highway sites of highest accident involvement. Kemper (6) reports that 43 percent of all two-lane traffic accidents in Virginia in 1965 involved overtaking and/or passing, approximately 50 percent of which might be attributable to skidding.

A skidding accident occurs when the maximum force which can be transmitted at the tire-pavement interface is exceeded. This occurs under several circumstances, including:

1. Inadequate tire-pavement frictional potential due to pavement surface wear or inadequate design.

2. Large water film thickness on the pavement due to poor pavement drainage.
3. Inadequate geometric design.
4. Poor vehicle and/or tire condition.
5. Driver error through inattention or carelessness.

The above list indicates general circumstances under which a skidding accident may occur. Each particular situation is the result of a complex interaction between the roadway, vehicle, tire, and driver. Several researchers have investigated these interactions by analyzing accident data in such a manner as to highlight specific highway and traffic parameters pertinent to the particular situation. Sabey (7) reports the results of a study completed in Great Britain where the percentage of wet-pavement accidents correlated in an inverse linear fashion with pavement skid resistance as measured with the British Pendulum Tester. Mahone (8) showed that the percentage of wet-pavement accidents could be related to Predicted Stopping Distance Number (PSDN). The PSDN is a measure of skid resistance characterized by the distance required for a vehicle to perform a full locked-wheel stop from a known initial speed. Mahone also found that for a pavement with a constant PSDN, the percentage of wet-pavement accidents decreased as traffic volume increased. This suggests again the relationship between skidding accidents and vehicle maneuvers.

In addition to highway and traffic parameters, the wet-pavement skidding accident rate is also a function of the local environmental conditions (i.e., rainfall intensity, mean ambient temperature, etc.). Giles (9) has shown that skidding accident rates change with the seasons of the year, being highest in the late summer and fall. This elevated accident rate is attributable to numerous factors, but most notably, the seasonal change in pavement surface condition.

The study of frictional requirements reported by Kummer and Meyer (4) was designed to establish minimum skid resistance levels for main rural highways. The study relied upon information regarding driver behavior, skidding accident experience, and the mechanics of the tire-pavement interface, to develop models for the establishment of frictional requirements. The important conclusions drawn from that study were; (1) the establishment of frictional requirements for a particular site should be based upon a statistical description of the traffic at that site, (2) frictional requirements can only be cost-effectively established with respect to the local demands established by traffic and (3) the upper bound upon the level of tire-pavement friction, which should be available to traffic, is determined by economic considerations, not by safety considerations.

Consistent with the conclusions, as described above, it is suggested that establishing the appropriate level of frictional requirements to reduce skidding accidents, should be accomplished by performing appropriate trade-offs between the desired level of safety (accident reduction), the costs associated with establishing that level, and the impacts on the level of service of the facility. The design level of friction is therefore not determined a priori, but is established by local policy as defined by the safety-cost-service tradeoff. In order to perform such tradeoffs, models are required which relate the key traffic operational, roadway geometric, pavement, and driver performance parameters to these measures.

The basis of the methodology is the hypothesis that the appropriate measure of safety is the difference between the level of available tire-pavement friction, F_A, and the level of demanded friction, F_D. Therefore models to estimate F_D and F_A as a function of operational, pavement and traffic parameters are required. Figure 2 is a flow chart of the major steps of the methodology. The methodology emphasizes that the level of demanded friction is dependent upon specific maneuvers and upon the frequency of occurrence of each maneuver. In addition, since several high frictional demand maneuver types may occur at a site, the methodology allows for the combination of the frictional demand for the individual maneuvers into an overall site frictional demand. A brief example is given to illustrate this point.

Consider a two lane isolated horizontal curve. The following maneuvers may occur (1) constant speed cornering, (2) cornering with acceleration, (3) cornering with braking, and (4) passing. The passing maneuver may be the most severe due to the combination of high longitudinal and lateral accelerations, however the frequency of occurrence of this maneuver may be low. Constant speed cornering has the lowest frictional requirement but the highest frequency of occurrence. The other two maneuvers are intermediate both in terms of severity and frequency. The friction required by drivers at the site is a function of the severity and frequency of occurrence of the maneuvers at the site, and is represented as a weighted average of the severity and the frequency of occurrence as follows:

$$(F_D)_T \sum_{i=1}^{n} \alpha i (F_D)_i \qquad (1)$$

where

$(F_D)_T$ = total frictional demand (SN_{40})

$(F_D)_i$ = frictional demand for ith maneuver (SN_{40})

α_i = frequency of occurrence of ith maneuver (Number/Day)

The completion of the methodology requires the development of models for estimating available tire-pavement friction, characterized by SN_{40}, and the level of demanded friction characterized by peak maneuver accelerations as a function of site variables. In addition, the means to compare available and demanded friction on a common scale as well as the prediction of maneuver frequencies is required.

Available Tire-Pavement Friction

The lack of general relationships for skid number and key parameters has prompted research directed towared characterizing the effect of the more important design parameters. A description of the influence of the key parameters on available tire-pavement friction, SN_{40}, is given in References (10 and 11). In this context recent work has been directed to the development of relationships between skid number and speed as shown below.

$$SN = SN_{40} + (SNG)\ V \qquad (2)$$

where

SN = skid number (a function of speed and pavement properties)

V = speed

SNG = skid number speed gradient (a function of pavement properties)

A qualitative description of the manner in which surface texture influences the skid number-speed curve has been reported (10, 11). It is generally accepted that while the shape and size of the pavement asperities determined, to a large degree, the hysteresis friction losses sustained by the tire, it is the channels between these asperities (i.e., pavement macrotexture) which facilitate the removal of the bulk water from the surface, and consequently determine the amount of dry contact area in the tire-pavement interface. The drainage characteristics of the pavement, therefore, directly affect the skid number-speed relationship since significant frictional forces can only arise in the dry contact area.

Schultze and Beckmann (12) report the development of a relationship between pavement drainage characteristics and the slope of the skid number-speed curve. Using stereophotographs of 48 pavement textures, it was shown that a correlation does exist between the mean void width of the pavement texture (i.e., the average spacing of pavement asperities) and the skid number-speed gradient. The results are given as Equation 3 and are shown in Figure 3.

$$Y = 14.5 \quad 72.6X \quad 103.6X^2 \qquad (3)$$

where

Y = mean void width (1/100 inch)

$X = SN_{20} = SN_{60}$ (speed in km/hr)

It should be noted that these results are based upon a sample of only 48 pavements and therefore must be applied carefully.

Equation 3 has been applied recently to the evaluation of the skid number speed gradient of a wide variety of in service pavements (13). Further verification of this relationship has been performed by comparing trends in the data reported by Gallaway (14) with those associated with Equation 3. The comparison has shown acceptable agreement, thus providing further confidence in the relationship.

For convenience to this application the original Schulze-Beckman correlation has been modified so that the parameters are expressed in standard units as follows:

define

$$X^* = \frac{SN_{12.5} - SN_{37.5}}{SN_{25}} \qquad (4)$$

and

$$X^* = 1.491 - \left\{-0.122 + 0.156y\right\}^{1/2} \qquad (5)$$

where

y = mean void width (1/100 inch)

More recently new instrumentation has been developed by which more detailed characterization of pavement characteristics is possible. Moore (15) measured the drainage characteristics of seven laboratory and roadway pavement samples using the Outflow Meter, an instrument which simply simulates the escape of water through texture canals in the tire-pavement contact area. Assigning a drainage number, based on relative drainage capability to each of the surfaces, a significant correlation was developed between the drainage numbers and the skid number-speed gradient. Substantial agreement exists between Moore's results and those of Schulze, and Beckmann, thus further confidence in these parameters as descriptors of SN_{40} is obtained. Equation 5 above will be the predictive relationship employed by the methodology.

Frictional Demand

Frictional demand associated with passing on two-lane rural roadways, and cornering on isolated horizontal curves, were studied experimentally within the study reported in Reference (11). Intersection braking, a high frictional demand maneuver, has been studied by Farber (16). Although the results of that study are employed in the methodology, for brevity, they are not discussed here.

Passing of Two-Lane Rural Roadways

Data was collected at four two-lane passing sites in Louisiana and California in order to characterize the relationship between combinations of lateral and longitudinal acceleration traffic parameters and site variables. The data consisted of time position measurements, which were converted to speed, lateral placement and longitudinal and lateral acceleration values. The site data is summarized below:

Summary of Passing Site Data

State	Route	File Number	Length (ft)	ADT	Sample Size
Louisiana	167	C3-1	> 3000	2180	18
Louisiana	167	C3-1	> 3000	2180	49
Louisiana	167	C3-3	> 3000	2180	38
California	121	T2-1	> 3000	5400	38

The experiments employed an impeding vehicle to encourage selected drivers to perform a passing maneuver. A schematic of the test scenario is given in Figure 4. The driver of the impeding vehicle (I) waits, at the roadedge, for a candidate passing vehicle (P). When an appropriate subject is identified an impeding vehicle pulls onto the roadway and establishes a predetermined impeding speed (Vi), (typically 35 to 45 mph). The passing vehicle after being captured and stabilized at speed Vi is maintained at that speed throughout the impeding section (typically 1/4 mile in length). Upon entering the instrumented test section, the impeded vehicle decides whether or not to pass. The time position signature of the passing maneuver is recoreded for later analysis. A typical recored is shown in Figure 5.

where:

X = distance along passing lane (ft)

Y = lateral position from roadedge (ft)

V = vehicle speed (mph)

ALONG = vehicle longitudinal acceleration (g)

ALAT = vehicle lateral acceleration (g)

RADV = vehicle path radius (ft)

Prior to a discussion of the detailed analysis of the passing data, it is appropriate to consider the general data trends. Figure 6 shows the one σ (one standard deviation) envelope of vehicle trajectories during passing. This figure was developed by referencing all lateral and longitudinal dimensions to the start of the passing maneuver. The transformed lateral coordinate Y_S, represents the lateral deviation of vehicle path during the passing maneuver.

It should be noted that the mean passing path deviation is 9.1 feet for the pullout portion of the maneuver. The 10 envelope represents a maximum distance which is approximately 0.5 to 0.75 of the average vehicle track width. Also note that the length of the pull out portion of the maneuver is approximately 400 feet.

Mean values for lateral acceleration, longitudinal acceleration, and vehicle speed are shown in Figure 7. This figure shows that vehicles tend to continue accelerating throughout the pullout and passing phase of the maneuver. The figure also suggests that critical combinations of lateral and longitudinal acceleration may exist.

The objective of this task was the development of relationships for the prediction of lateral and longitudinal acceleration levels during the passing maneuver. Since individual site sample sizes were insufficient, data from all sites were lumped for analysis. A series of analyses were performed to determine if relationships with the general form of Equations 6-10 could be developed from the data.

$$ALATM = J_i ALON\ GA + K_j \quad (6)$$

$$ALATM = K_i ALONGM + K_j \quad (7)$$

$$ALATM = K_i SPD + K_j \quad (8)$$

$$ALONGM = K_i GAP + K_i \quad (9)$$

$$ALATM = K_i RA + K_i \quad (10)$$

where

ALATM = maximum lateral acceleration (g)

ALONGA = longitudinal acceleration associated with ALATM (g)

ALONGM = maximum longitudinal acceleration (g)

SPD = vehicle speed at the first trap (mph)

GAP = passing gap (ft)

RA = vehicle path radius associated with ALTM (ft)

No correlation was found to exist between ALATM and any of the dynamic variables (equation 6 to 9) however, significant correlation was found to exist between ALATM and the associated vehicle path radius, RA (Equation 10). This relationship is shown for selected data in Figure 8 and given below,

$$ALATM = \frac{170}{RA} \quad (11)$$

Analysis of data collected by Glannon (17) during a program conducted at Texas Transportation Institute indicates a similar relationship for maximum lateral acceleration. These results are given in Figure 9.

Although the data trends exhibited by Figure 8 and 9 are the same, the magnitude of the maximum lateral accelerations are different. The data collected by Glennon was designed to address high speed passing maneuvers where impeding vehicle speeds were in excess of 50 mph. The data collected in this study was designed to address a more naturally occurring range of impeding speeds, 35 mph to 50 mph. The relationship given in Equation 11 is believed more responsive to this problem, and therefore, will be utilized as the basis for establishing passing frictional requirements.

In order to establish the level of frictional demand for the passing maneuver, the level of longitudinal acceleration and speed associated with ALATM are required. A Kilmogorov-Smirnov 2 tailed test was conducted to establish the normality of (1) the distribution of longitudinal acceleration associated with ALATM (2) the distribution of speed associated with ALATM and (3) the distribution of RA associated with ALATM. Each distribution was found to be normal at the 5 percent level. A similar analysis established that the distribution of ALATM was not normal.

Since the value of RA is not an easily measurable quality, it cannot conveniently be utilized parametically. However, following the analyses performed by Glennon (17) RA can be utilized as a desing guide by calculating the value of ALATM associated with various cumulative percentile levels of RA. Glennon, for example chose the 10th percentile (the value of RA such that 10 percent of the vehicles had path radii smaller than RA) as the design point.

In order to determine the total frictional demand, values of longitudinal acceleration and speed must be calculated in a manner consistent with the choice for cumulative percentile of RA. It is recommended that the following set of predictors be utilized.

$$\left.\begin{aligned} ALATM_p &= \frac{170}{RA_p} \\ RA_p &= \overline{RA} + Z_p \sigma R \\ ALONGA_p &= \overline{ALONGA} + Z_p \sigma_A \\ VA_p &= \overline{VA} + Z_p \sigma_V \end{aligned}\right\} \quad (12)$$

where

ALATM = maximum lateral acceleration (g)

RA = vehicle path radius associated with ALATM (ft)

$\overline{RA}$ = mean of RA (ft)

σ_R = standard deviation of RA (ft)

ALONGA = longitudinal acceleration associated with ALATM (g)

$\overline{ALONGA}$ = mean of ALONGA (g)

σ_A = standard deviation of ALONGA (g)

V_p = vehicle speed associated with ALATM (mph)

$\overline{VA}$ = mean of VA

σ_V = standard deviation of VA

Z = normal distribution parameter

P = subscript denoting cumulative percentile level

Passing Frequency

A model has been developed to predict the expected frequency of passes on a two-lane rural road as a function of traffic distribution, speed, and driver behavioral characteristics. The model incorporates past passing behavioral research into an intuitive model and is given in Equation 13 below:

$$\dot{N}_p = \sum_{i=1}^{r} (k_i L) \sum_{j=i+1}^{r} k_j (v_j - v_i) \cdot \int_{x=o}^{\infty} \alpha(x(v_j - v_i))\, \hat{\phi}(x)\, dx \tag{13}$$

where

$\dot{N}_p$ = frequency of passing (no./mile-hr)

k = concentration of vehicles (no./mile)

L = section length (mile)

V = speed (mph)

α = gap acceptance function

x = passing gap

$\hat{\phi}$ = distribution of inter-arrival times $(ft)^{-1}$

In order to calculate the expected frequency of passing of a particular section of roadway, models for the gap exceptance function must be developed. Farber (18) has measured the gap acceptance function under conditions similar to the ones utilized for testing in this program. Utilizing this data, a model has been developed to fit the gap exceptance data. This model is of delayed exponential form, and is given by the following:

$$\alpha(x,\Delta V) = \begin{cases} 0 & \text{if } x < x_L(\Delta V) \\ 1 - e^{-\theta(x-x)_L} & \text{if } x \geq x_L(\Delta V) \end{cases} \tag{14}$$

where for convenience $(v_j - v_i)$ is denoted by ΔV. Assuming that the dependence of $\alpha(x,\Delta V)$ on ΔV is only due to dependence of x_L on ΔV and the dependence of x_L on ΔV is linear, and further assuming that the distribution of inter-arrival time $\hat{\phi}(x)$ is exponentially distributed with rate λ, a closed form integration can be performed to determine values of $x(\Delta V)$. The results of this integration are given below:

$$\alpha(\Delta V) = \frac{\theta}{\theta+\lambda} e^{-\hat{\lambda} x_L} \tag{15}$$

For convenience, various values of the gap acceptance function have been tabulated for traffic flow rates in the oncoming lane of 500 vehicles per hour at a rate of arrival in the passing lane of 0.12 per second. These are shown in Table 1. Based upon the calculated gap acceptance function in Table 1, estimations of the number of passings which will occur on a given section of roadway can be made. An example follows:

Assume that there are two distinct speed bins, V_1 = 30 mph and V_2 = 50 mph and q, q_1, q_2 denote the volume of vehicles, vehicles having Speed V_1 and vehicles having speed V_2, respectively. Also assume that $q_1 = q_2$ and that $q_i = k_i v_i$ where i = 1,2. Then the number of passings of vehicles per hour for L = 0.1 mile is calculated for various values of q and $\hat{\lambda}$. It has again been assumed that θ = 0.12 per second, and $\alpha(v_j - v_i)$ is given in Table 1. The calculations are summarized in Figure 10. The passing frequency model, Equation 13 will be utilized in the development of site frictional requirements.

Constant Speed Cornering

Data was collected at 9 isolated horizontal curves in Louisiana, Mississippi and California in order to characterize the relationship between lateral acceleation, traffic parameters and site variables. The data consisted of time position measurements which were converted to speed, lateral placement and lateral acceleration values. The site data is summarized in Table 2.

The data were analyzed according to the analysis scheme originally outlined by Farber (16). However, normality tests indicated in general that, on a trap by trap basis, peak lateral acceleration, and speed were not distributed normally. Therefore, a series of direct regressions were performed for all sites combined with the following results:

$$A_{p,99} = 2.424\, \bar{A}_{NOM} + 1.097\, \sigma_{NOM} - \frac{295.349}{R} + 0.339 \tag{16}$$

$$A_{p,95} = 2.209\, \bar{A}_{NOM} + 0.617\, A_{N,95} - \frac{285.247}{R} + 0.240 \tag{17}$$

$$A_{p,90} = 2.426\, \bar{A}_{NOM} + 0.472\, \bar{A}_{N,90} - \frac{247.145}{R} + 0.184 \tag{18}$$

$$V_{p,99} = 1.017\, \bar{V}_N + 0.829\, \sigma_N - \frac{1101.721}{R} + 7.611 \tag{19}$$

$$V_{p,95} = 0.914\, \bar{V}_N + 0.804\, \sigma_N - \frac{978.017}{R} + 8.366 \tag{20}$$

$$V_{p,90} = 0.909\, \bar{V}_N + 0.777\, \sigma_N - \frac{743.765}{R} + 7.654 \tag{21}$$

where

$A_{p,99}$ = 99th percentile peak acceleration (g)

$A_{p,95}$ = 65th percentile peak acceleration (g)

$A_{p,90}$ = 90th percentile peak acceleration (g)

$\bar{A}_{NOM}$ = mean nominal acceleration, $V^2/15R$ (g)

σ_{NOM} = standard deviation of nominal acceleration distribution (g)

R = site radius of curvature (ft)

$A_{N,95}$ = 95th percentile of nominal acceleration distribution (g)

$V_{p,99}$ = 99th percentile peak velocity (mph)

$V_{p,95}$ = 95th percentile peak velocity (mph)

$V_{p,90}$ = 90th percentile peak velocity (mph)

$\bar{V}_N$ = mean nominal speed distribution (mph)

σ_N = standard deviation of nominal speed distribution (mph)

These equations are utilized to estimate the specified levels of acceleration demand as a function of speed values measured at the midpoint of the curve as follows

$$A_{NOM} = \frac{V_{mp}^2}{15R} \tag{22}$$

$$V_{NOM} = V_{mp} \tag{23}$$

Relationship Between Acceleration and Skid Number

The problem of relating combinations of longitudinal and lateral accelerations developed by a vehicle to resultant vehicle acceleration and pavement skid number, including the effects of vehicle dynamics, vehicle configuration and tire properties, remains unresolved in general. Many attempts have been made to develop simple relationships between these quantities. In particular, the following relationship has been used widely

$$ARES = \left(ALAT^2 + ALONG^2\right)^{1/2} \tag{24}$$

where

ARES = resultant acceleration (g)

ALONG = longitudinal acceleration (g)

ALAT = lateral acceleration (g)

This relationship is an approximation to a more general relationship which describes the resultant acceleration in terms of the combination of lateral and longitudinal acceleration in elliptical form as follows:

$$\left(\frac{ALONG^2}{ALONGM^2} + \frac{ALAT^2}{ALATM^2}\right)^{1/2} = 1 \tag{25}$$

where

ALONG = longitudinal acceleration (g)

ALONGM = maximum longitudinal acceleration (g)

ALATM = maximum lateral acceleration (g)

ALAT = lateral acceleration (g)

Data developed at the Texas Transportation Institute and reported by Hayes (17) indicates that the single mode maxima of the longitudinal acceleration and lateral acceleration can be related to speed and SN_{40}. These results are shown in Figure 11. These data were collected during full-scale test track experiments where a single vehicle was maneuvered under a variety of speeds on several different pavement types and the accelerations monitored on-board in the vehicles.

The thrust of the results shown in the figure is that bounding values of combinations of longitudinal and lateral acceleration can be determined as a function of speed and skid number. Although it is not entirely clear from this data that unique correlations between dynamic variables and SN_{40} exist, the limited results thus far do indicate that the bounds can be established for specific pavement types.

Although no universal correlation between SN_{40} and combinations of longitudinal and lateral acceleration has been demonstrated, the formulation shown in Figure 11 has been in widespread use. The original formulation was introduced by Harris and Reilly (18) and subsequently used extensively by Holmes and Stone (19). Also, these relationships form the basis for calculating the coefficient of friction, at the tire-pavement interface, in large scale simulation models including HVOSM (20).

Farber (16) had developed limited data of this kind for one vehicle type. This data is shown in Figure 12, where the skidding bounds are indicated by the best fit ellipse.

The form of the available data is such that it is more convenient to convert SN_{40} levels to equivalent acceleration values utilizing the previous figure. The procedure to accomplish this is based upon a determination of the radius of a circle which passes through the point (ALAT*, ALONG*). These points represent the calculated values of longitudinal and lateral acceleration demand. The resultant acceleration (ARES) corresponding to the specific SN_{40} value is given below

$$ARES^2 = ALATM^2 + (ALONG^*)^2 \left[1 - \left(\frac{ALATM^2}{ALONGM^2}\right)\right] \tag{26}$$

where

ARES = resultant acceleration corresponding to SN_{40} (g)

ALATM = maximum lateral acceleration corresponding to SN_{40} (g)

ALONGM = maximum longitudinal acceleraiton corresponding to SN_{40} (g)

ALONG* = calculated longitudinal acceleration demand (g)

The balance between the level of acceleration demand (ARESD)(combination of lateral and longitudinal ma, acceleration) and available tire pavement friction (ARBSA) is evaluated by calculating ARES and described above and comparing that with the level of acceleration demand calculated using Equation 16. A set of example calculations

utilizing the data contained in Figure 12 is given in Table 3 also note that the normalized margin of available function over demanded friction is also tabulated. Positive values of the margin imply no skidding.

Utilizing the relationships developed for available tire-pavement friction and the level of demanded friction, the margin of safety can be calculated as their difference as a function of traffic, operational and pavement properties.

As discussed previously, the goal of the methodology development is to provide a tool by which cost, safety, and service considerations can be traded off to establish frictional requirements consistent with local policy guidelines. The concept of this trade-off analysis is shown in Figure 12. In the context of this discussion, the safety parameter, S is given by MOS, the costs are those attributable to establishing the level of safety, and the level of Service, F, is defined in the standard engineering sense by speed and delay.

Conceptually, the trade-off problem is one of simultaneously satisfying multiple objectives for S, C, and F. However, practically the problem is reduced to a single objective problem with constraints. Consider the example in Figure 13.

Suppose the objective is to maintain the cost within the bounds C_1 and C_2 with the constraint that the level of safety should be maintained between S_1 and S_2 and the level of service should be between F_1 and F_2. In addition, it is postulated that there is a bonding relationship between cost and service given by $C = f(F)$. Under these circumstances the skidding accident reduction countermeasures which satisfy these constraints are shown by the shaded region. Several other interesting points can be noted. Point B_2 is the solution for highest level of safety; point B_5 is the solution for lowest cost, and point B_4 is the point of diminishing returns.

In summary, the establishment of cost-effective frictional requirements is a policy issue which requires tools to consider the interaction of highway, vehicle, driver, and environmental factors at specific highway sites. The detailed application of the methodology requires the development of continuous frictional relationships between the variables. Such relationships have not as yet been developed.

References

1. R.L. Rizenbergs, J.L. Burchett, C.T. Napier, "Accidents on Rural Interstate and Parkway Roads and Their Relation to Pavement Friction," Kentucky Department of Transportation, Bureau of Highways, Research Report No. 377, October 1973.
2. "Accidents and the Human Element in Skidding," Final Report of Subcommittee B, First International Skid Prevention Conference, Highway Research Record No. 219, 1959.
3. K.D. Hankins, et al, "Influence of Vehicle and Pavement Factors on Wet-Pavement Accidents," Highway Research Record No. 376, pp. 66-84, 1972.
4. H.W. Kummer, W.E. Meyer, "Tentative Skid-Resistance Requirements for Main Rural Highways," NCHRP Report 37, 1967.
5. H.A. Smith, "Pavement Skid Resistance Requirements," paper prepared for Review of Federally Coordinated Program, Estes Park, Colorado, July 1973.
6. W.J. Kemper, P.E. Huntington, S.R. Byington, "Over-Taking and Passing Vehicle Accidents," Public Roads, Vol. 37, No. 3, pp. 81-88, 1972.
7. B.E. Sabey, "Road Surface Characteristics and Skidding Resistance," Journal of British Granite and Whinstond Federation, Vol. 15, No. 2, 1965.
8. D.C. Mahone, S.H. Runkle, "Pavement Friction Needs," Highway Research Record No. 396, pp. 1-11, 1972.
9. C.G. Giles, B.E. Sabey, "A Note on the Problem of Seasonal Variation in Skidding Resistance," Proceedings of the First International Skid Prevention Conference, Virginia Highway Research Council, Part 2, 1958.
10. J.M. Zuieback, et al., "Frictional Requirements Necessary to Reduce Skidding Accident Frequencies - Interim Report," prepared for U.S. Department of Transportation, by Science Applications, Inc., Report No. SAI-74-542-LA, August 1974.
11. J.M. Zuieback, et al., "Frictional Requirements Necessary to Reduce Skidding Accident Frequencies Final Report," prepared for the U.S. Department of Transportation by Science Applications, Inc. Report No. SAI-260-77-547-LA, January 1977.
12. K.H. Schulze, L. Beckman, "Friction Properties of Pavements at Different Speeds," ASTM Special Technical Publication 326, pp. 42-49.
13. "Effectiveness of Alternative Skid Reduction Measures Interim Report No. 2," prepared for U.S. Department of Transportation, by Midwest Research Institute, MRI Project No. 3824-E, July 1975.
14. B.M. Gallaway, J.G. Rose, "Macro-Texture, Friction, Cross Slope and Wheel-Track Depression Measurements on 41 Typical Texas Highway Pavements," Texas Transportation Institute, Research Report No. 138-7, Texas A&M University, June 1970.
15. D.F. Moore, "Prediction of Skid-Resistance Gradient and Drainage Characteristics for Pavements," Highway Research Record No. 131, pp. 181-203, 1966.
16. E. Farber, et al., "Pavement Friction Coefficients for Driving Tasks," prepared for Highway Research Board, Project 1-12, by the Franklin Instrument Research Laboratories, April 1973.
17. G.G. Hayes, "Tire-Pavement Friction as a Function of Vehicle Maneuvers," Texas Transportation Institute Report 163-wF, NTIS PB 240 269, 1974.
18. A.J. Harris, B.S. Riley, "Vehicle Behavior in Combined Cornering and Braking," Proceedings Institute of Mechanical Engineers, Vol. 183, Pt. 3H, 1969.
19. K.E. Holmes, R.D. Stone, "Type Forces in Combined Cornering and Braking Slip on Wet Road Surfaces," Road Research Laboratory, RRL Report LR 254, 1969.
20. R.R. McHenry, "An Analysis of Dynamics of Automobiles During Simultaneous Cornering and Ride Motions," Proceedings Institute of Mechanical Engineers, Vol. 183, Pt. 3H, 1969.

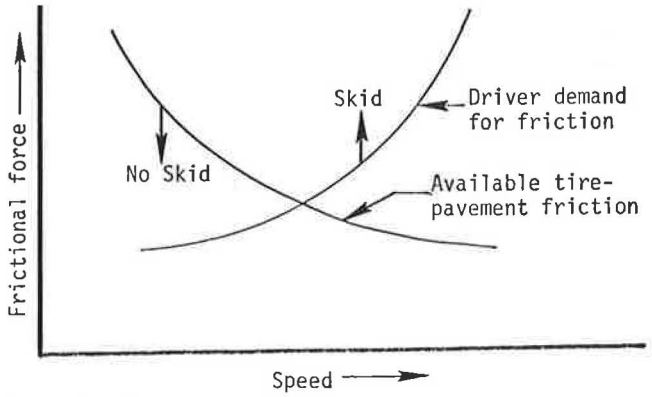

Figure 1. Relationship between available tire-pavement and driver demand for friction.

Figure 2. Flow chart.

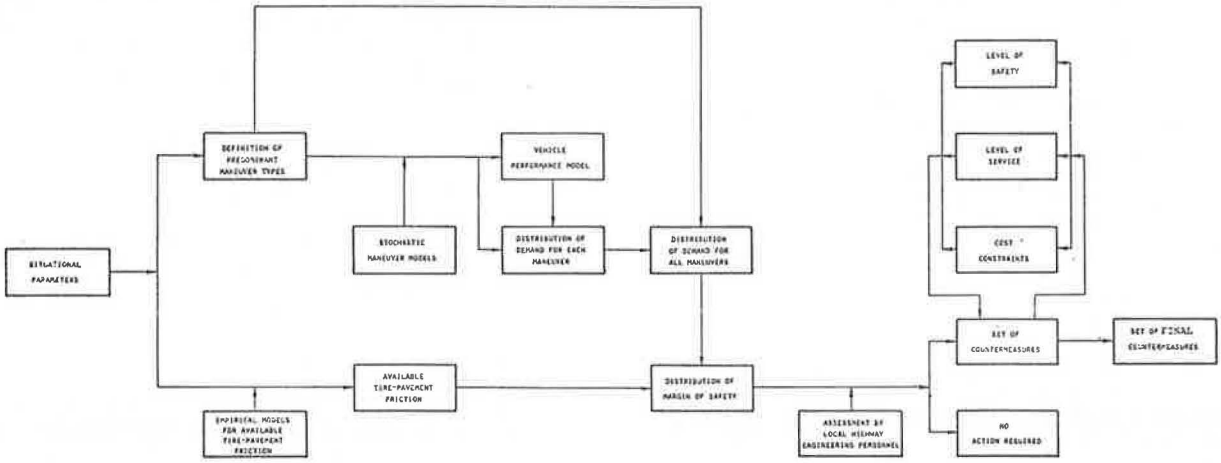

Figure 3. Correlation between surface texture and friction coefficient-speed gradient.

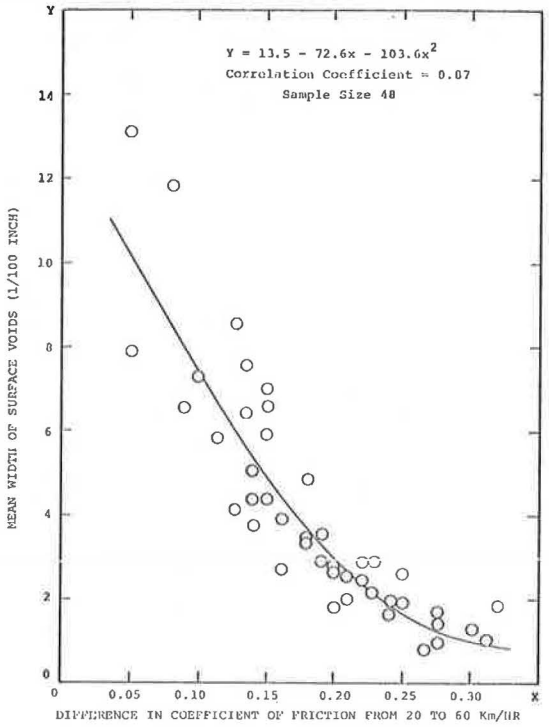

Figure 4. Example of passing scenario using impeding vehicle.

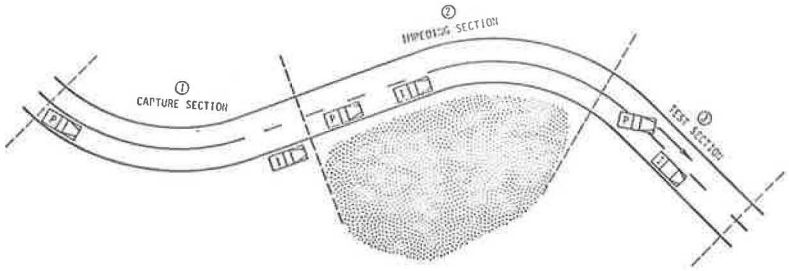

Figure 5. Sample processed passing record.

TRAP	X	POS	Y	SPD
1	0.0	9.74	9.89	41.01
2	45.0	10.19	10.36	42.41
3	90.0	11.15	11.20	46.53
4	135.0	12.25	12.65	46.22
5	180.0	14.58	14.58	49.59
6	225.0	16.96	16.94	50.04
7	270.0	14.66	19.06	54.55
8	315.0	16.26	20.44	50.51
9	360.0	0.00	21.09	0.00
10	405.0	16.60	21.11	56.52
11	450.0	16.34	20.76	0.00
12	495.0	15.37	19.13	59.29
13	540.0	0.00	17.92	0.00
14	585.0	17.36	16.34	61.63
15	630.0	15.30	15.23	61.63
16	675.0	13.02	13.02	62.34
17	720.0	10.73	11.49	62.70
18	0.0	0.00	10.73	0.00
19	0.0	0.00	10.73	0.00
20	0.0	0.00	10.73	0.00

V	ALNG	ALAT	RADV
41.54	0.000	0.000	0.
42.72	.092	.022	5.525E+03
44.45	.134	.040	3.305E+03
46.78	.144	.035	4.170E+03
48.62	.166	.033	4.856E+03
51.39	.117	-.020	8.837E+03
51.70	.056	-.046	2.706E+03
52.86	.071	-.047	2.782E+03
53.51	.124	-.059	3.267E+03
55.98	.182	-.039	5.529E+03
57.90	.139	-.141	1.508E+03
59.22	.112	.008	4.808E+03
60.46	.091	-.044	5.582E+03
61.24	.064	.057	4.408E+03
61.87	.045	-.138	1.853E+03
62.22	.033	.087	2.957E+03
62.58	0.000	0.000	0.
62.70	0.000	0.000	0.
62.70	0.000	0.000	0.
62.70	0.000	0.000	0.

Figure 6. Distribution of mean passing paths for sites in Louisiana and California.

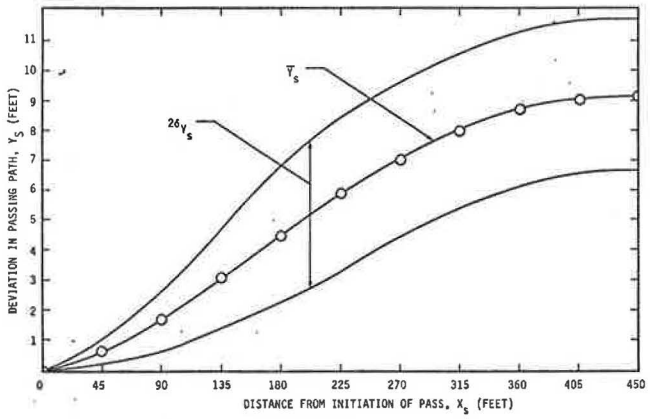

Figure 7. Distance from initiation of pass, Xs (feet).

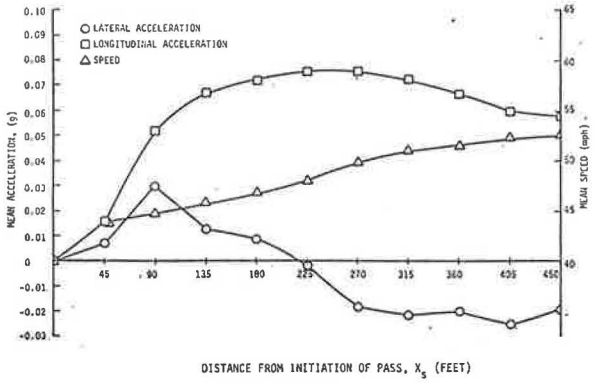

Figure 8. Relationship between maximum lateral acceleration and path radius during passing.

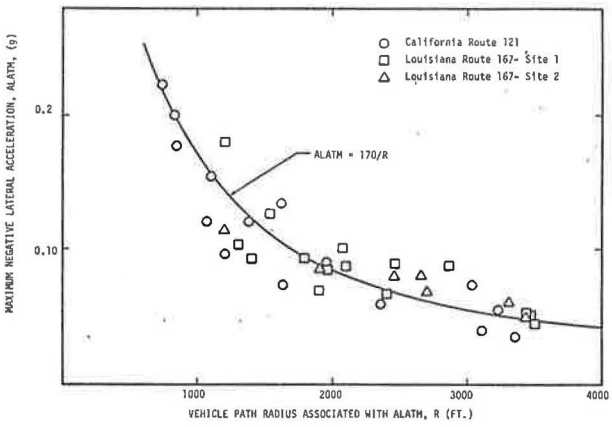

Figure 9. Relationship between lateral acceleration and path radius during passing.

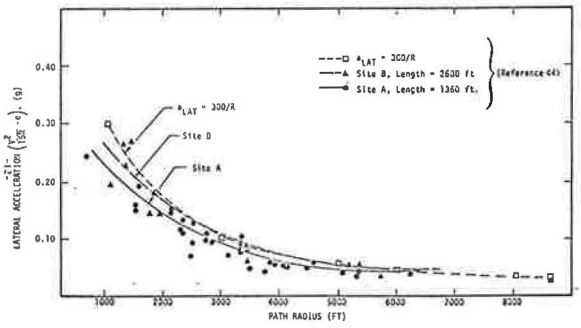

Table 1. Tabulations of the gap acceptance function.

x (sec)	ΔV = 29 mph x_L = 6.0 sec α(x,ΔV)	ΔV = 15 mph x_L = 6.5 sec α(x,ΔV)	ΔV = 10 mph x_L = 7.0 sec α(x,ΔV)	ΔV = 5 mph x_L = 7.5 sec α(x,ΔV)
< 6.0	0	0	0	0
6.5	.058	0	0	0
7.0	.133	.058	0	0
7.5	.165	.113	.058	0
8.0	.213	.165	.113	.058
10.0	.381	.343	.302	.259
12.0	.532	.483	.451	.417
14.0	.617	.593	.568	.542
16.0	.698	.680	.660	.639
18.0	.763	.748	.732	.716
20.0	.813	.802	.790	.777
22.0	.853	.844	.834	.824
24.0	.884	.877	.870	.862
26.0	.909	.904	.898	.891

Figure 10. Rate of passing for various q's and $\hat{\lambda}$'s.

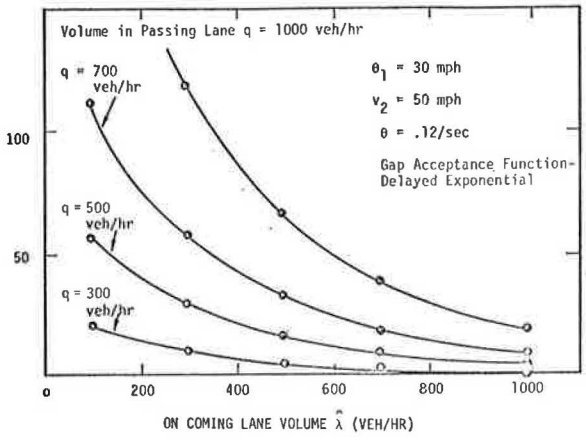

Table 2. List of test sites.

Location	Site No.	Type	Direction of Traffic	Days of Observation	Pavement Condition	Radius of Curvature	ADT
Mississippi							
US 98 Map Section 1375	C9-1	Curve	Both	#1	Dry	1432	1900
US 98	C9-1	Curve	Both	#2	Wet	1432	1900
SR 48 Map Section 260	CB-1	Curve	Both	#1	Dry	1087	1540
SR 48	CB-1	Curve	Both	#2	Dry	1087	1540
Louisiana							
US 167 MP 131	C3-5	Curve	Northbound	#1	Wet	2864	2180
US 167 MP 131	C3-5	Curve	Northbound	#2	Dry	2864	2180
US 167 MP 131	C3-5	Curve	Southbound	#1	Dry	2864	2180
US 167 MP 138	C3-2	Curve	Southbound	#1	Dry	2864	2180
US 167 MP 138	C3-2	Curve	Southbound	#2	Wet	2864	2180
US 167 MP 138	C3-2	Curve	Northbound	#1	Dry	2864	2180
California							
SR 88 MP 7.9	C22-3	Curve	West	#1	Dry	1210	1500
SR 88 MP 7.9	C22-3	Curve	East	#1	Dry	1210	1500
SR 88 MP 10	C22-2	Curve	West	#1	Dry	3200	1500
SR 88 MP 10	C22-2	Curve	West	#1	Wet	3200	1500
SR 121 MP 2.31	C2-4	Curve	East	#1	Dry	1400	7400

Figure 11. Relationship between acceleration SN_{40} and speed.

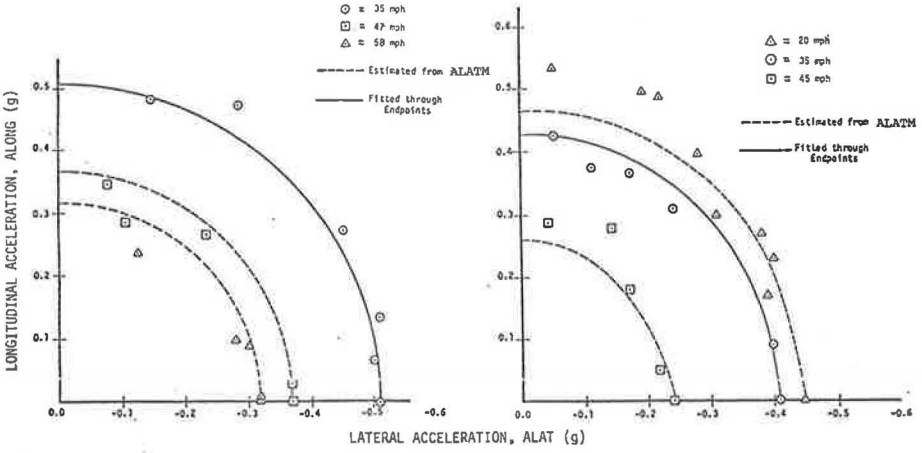

Figure 12. Maximum forward acceleration as a function of lateral acceleration.

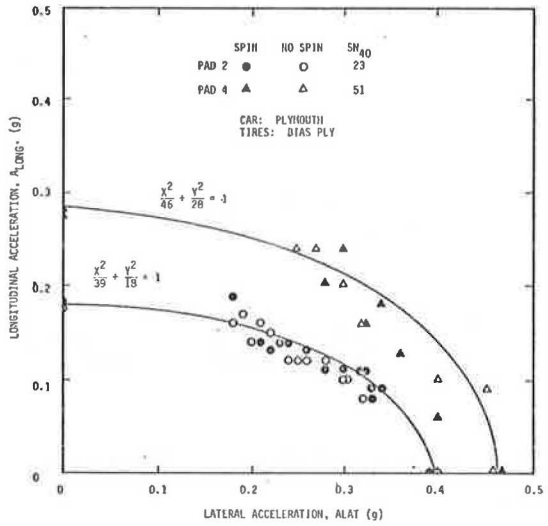

Table 3. Sample calculations for frictional demand and available pavement friction

DEMAND			AVAILABLE MARGIN		
ALAT (g)	ALONG (g)	ARESD (g)	SN_{40}	ARESA (g)	ARESA-ARESD AR2SA
0.2	0.1	0.22	23	0.34	0.35
			51	0.44	0.50
0.2	0.15	0.25	23	0.26	0.04
			51	0.42	0.40
0.2	0.2	0.28	23	0.07	-3.0
			51	0.38	0.26
0.2	0.25	0.32	23	-	-
			51	0.33	0.03
0.25	0.1	0.27	23	0.34	0.21
			51	0.44	0.39
0.25	0.15	0.29	23	0.26	-0.12
			51	0.42	0.31
0.25	0.20	0.32	23	0.07	-3.6
			51	0.38	0.16
0.25	0.25	0.35	23	-	-
			51	0.33	-0.06
0.30	0.10	0.32	23	0.34	0.06
			51	0.44	0.27
0.30	0.15	0.34	23	0.26	-0.31
			51	0.42	0.19
0.30	0.20	0.36	23	0.07	-4.1
			51	0.38	0.05
0.30	0.25	0.39	23	-	-
			51	0.33	-0.18
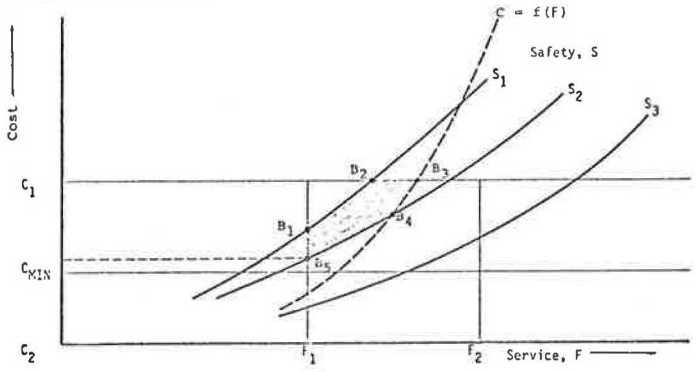
Figure 13. Concept of the trade-off analysis for cost, safety, and service